Journal of
Analytical & Bioanalytical Techniques

Shirmanova et al., J Anal Bioanal Tech 2014, S1
DOI: 10.4172/2155-9872.S1-008

Research Article Open Access

Comparative Study of Tissue Distribution of Chlorin e6 Complexes with Amphiphilic Polymers in Mice with Cervical Carcinoma

Marina V Shirmanova[1,2]*, Alena I Gavrina[1,2], Nadeshda A Aksenova[3], Nikolay N Glagolev[3], Anna B Solovieva[3], Boris E Shakhov[1] and Elena V Zagaynova[1,2]

[1]*Nizhny Novgorod State Medical Academy, Minin and Pozharsky, Russia*
[2]*Lobachevsky State University of Nizhny Novgorod, Russia*
[3]*Semenov Institute of Chemical Physics RAS, Russia*

Abstract

Many photosensitizers, including chlorins, are highly hydrophobic, which makes intravenous administration problematic and affects their delivery to the tumor and uptake in the cells. Moreover, self-aggregation of the photosensitizer in aqueous solution reduces fluorescence quantum yield, triplet state, and singlet oxygen generation, and consequently diminishes photosensitizing activity. To address these issues, it was proposed to use biocompatible water-soluble polymers. However, animal studies of the photosensitizer-polymer systems are still very limited. In this work, polyvinylpyrrolidone (PVP), polyvinyl alcohol (PVA), and pluronic F108 were used for dissolution of chlorin e6 (Ce6). Dynamics of accumulation of the formulations in a mouse cervical carcinoma and clearance from normal tissue, drug plasma concentrations and tissue distribution after intravenous injection were investigated. Ce6 alone and clinically used photosensitizer Photoditazine served as a control. The results showed that none of the polymers significantly changed fluorescence kinetics in the tumor. Concentration of the Ce6 formulated with polymers in the tumor tissue was comparable with Photoditazine, but uptake in the skin was less. At the same time, tumor-to-skin ratios of the Ce6-polymer complexes were similar to free Ce6. We concluded that the use of the polymeric formulation is reasonable for fluorescence diagnosis and PDT of cancer.

Keywords: Photosensitizer; Chlorin e6; Amphiphilic polymer; PDT; Mouse cervical carcinoma; Fluorescence imaging *in vivo*; Chemical extraction

Introduction

Photodynamic therapy (PDT) is known to be a prospective modality for cancer treatment [1]. A regular PDT includes laser irradiation of the tumor following a systemic injection of the photosensitive dye – a photosensitizer (PS) that preferentially accumulates in the neoplastic tissue. Under the light exposure and in the presence of oxygen, the PS produces reactive oxygen species (ROS) destructive for the tumor [2].

For successful clinical application, PS should meet a few general requirements. Particularly, it should be water-soluble to be injected intravenously, have strong absorption in the red or near-infrared region for deeper penetration into tissue, have high singlet oxygen generation (SOG) quantum yield and low dark cytotoxicity, selectively accumulate in the tumor and weakly in the skin, and can be rapidly eliminated from the body.

A number of PSs of porphyrin and non-porphyrin structure have been designed by now [3]. Among them, chlorins are promising agents for PDT due to absorption and emission in the red spectrum range (around 660 nm), where the light penetrates deep enough into the tissues, high phototoxicity resulting in usage of low drug and light doses, rapid accumulation in tumor, and short skin photosensitivity. There are several chlorin-type photosensitizers in clinical use today – Temoporfin (Foscan, mTHPC, 5,10,15,20-Tetra(m-hydroxyphenyl) chlorin), Talaporfin (LS11, MACE, N-aspartyl chlorin e6, NPe6), Radachlorin (a mixture of three chlorins), and Photodithazine (glucosamine salt of chlorine e6) [4,5].

However, many PSs, including chlorins, are highly hydrophobic, which makes intravenous (i.v.) administration problematic and affects their delivery to the tumor and uptake in the tumor cells. Moreover, self-aggregation of PS in aqueous solution reduces fluorescence quantum yield, triplet state, and singlet oxygen generation, and consequently diminishes photosensitizing activity. Therefore, efficient drug delivery systems are highly needed to improve photophysical and pharmacokinetic parameters of PS.

Utilizing biocompatible water-soluble polymers can potentially solve the above mentioned problems. The PS-polymer systems based on non-covalent or chemical conjugation of hydrophobic PS with hydrophilic polymer such as polyethylene glycol (PEG) [6], polyvinylpyrrolidone (PVP) [7-11], polyvinyl alcohol (PVA) [12], have been described. Polymeric micelles are also considered as a promising system for PS delivery in PDT [13]. Micelle-forming polymers used for PS encapsulation include pluronics F127 [14] and P123 [15,16], [methoxy poly (ethylene glycol)-b-poly (caprolactone)] diblock copolymers (MePEG5000-b-PCL4100) [17], polyethylene glycol/phosphatidyl ethanolamine conjugate (PEG-PE) [18].

PS in the polymeric formulations has been shown to have an enhanced fluorescence quantum yield and generate more singlet oxygen due to disaggregation of PS and prevention of photobleaching [11,14,16]. Besides, a polymer is able to improve the permeation of the PS through cellular membranes [10,14]. *In vitro* studies on cancer

***Corresponding authors:** Marina V Shirmanova, PhD, Head of Laboratory, Nizhny Novgorod State, Medical Academy, Sq. Minin and Pozharsky, 10/1, Nizhny Novgorod, 603005, Russia, Tel: +7 831 465 4113; Fax: +7 831 465 4223; E-mail: shirmanovam@mail.ru

Received April 25, 2014; **Accepted** June 12, 2014; **Published** June 17, 2014

Citation: Shirmanova MV, Gavrina AI, Aksenova NA, Glagolev NN, Solovieva AB, et al. (2014) Comparative Study of Tissue Distribution of Chlorin e6 Complexes with Amphiphilic Polymers in Mice with Cervical Carcinoma. J Anal Bioanal Tech S1: 008. doi:10.4172/2155-9872.S1-008

cells demonstrate enhanced cellular internalization and photodynamic activity of Ce6 conjugates with PVP, Ce6 in pluronics micelles and PpIX in MePEG5000-b-PCL4100 micelles [4,14,19]. Finally, the polymers may increase accumulation of the PS in the tumor as a result of combination of the enhanced permeability and retention (EPR) effect with the longer systemic circulation properties [20]. However, very few chlorine-polymer systems have been examined in biological studies on tumor models *in vivo* to date [6,8,9,14].

It is known that a number of factors influence PS biodistribution and pharmacokinetics in animal body including those related to the PS (molecular weight, charge, formulation etc.) and design of the experiment (drug dose, administration route, tumor model), which makes it difficult to compare the results of different studies.

Therefore, the applications of the PS-polymer systems to fluorescence diagnostics and PDT are not widely explored. The only clinically approved polymer-based formulation with chlorin is Fotolon composed of chlorine e6 and PVP [21,22].

In this work, a comparative study of Ce6, three Ce6-polymer systems and Photodithazine (PDZ) has been performed. PVP, PVA, and pluronic F108 have been used for dissolution of Ce6. Dynamics of accumulation of the PSs in a mouse cervical carcinoma and clearance from normal tissue after i.v. injection have been investigated *in vivo* using fluorescence imaging. At the same time plasma concentrations of PS have been measured. Based on the *in vivo* imaging data and the plasma drug level, the time point at 4 h post-injection has been chosen for quantitative biodistribution analysis, and the amounts of PS in the tumor and normal tissues have been estimated by the chemical extraction method.

Experimental

Photosensitizers and polymers

The chemicals used in the study were chlorin e6 (Frontier Scientific, USA), polyvinylpyrrolidone (Dr. Theodor Schuchardt, Germany, Mw 25,000), polyvinyl alcohol (Sigma-Aldrich, USA, Mw 30,000), pluronic F108 - block copolymer of ethylene- and propylene oxide (Basf, USA, Mw 14,600).

Chlorin e6 (6 mg/mL) was dissolved in the water solution of $NaHCO_3$ (7.3 mg/mL). The polymer solution (10 mg/mL) was prepared separately. The solutions of polymer and chlorine were mixed in volume ratio 1:1 and incubated at ambient temperature for 15 min, so the chlorine concentration was 3 mg/mL, and polymer concentration was 5 mg/mL. The binding of the total Ce6 molecules in the complexes was 60-80% [19].

Photodithazine, water soluble N-methyl-D-glucosamine derivative of Ce6, was obtained from VetaGrand, Russia, at the concentration of 5 mg/mL.

Tumor model

All animal studies were approved by the Animal Care Committee at the Nizhny Novgorod State Medical Academy. The experiments were performed on female CBA mice (8-12 weeks old) obtained from the Nursery for laboratory animals (IBCH RAS, Pushchino, Russia). The total number of animals used in experiments was 38.

Transplantable mouse cervical carcinoma RShM-5 was obtained from the Blokhin Cancer Research Center (Moscow, Russia). The tumor model originated from MX-induced carcinoma of cervix uteri was introduced in experimental oncology in Russia in the late 1970s [23]. Subcutaneous tumors were generated by injecting 20 mg tumor tissue dissociated into single cell suspension and suspended in 180 µl of Medium 199 (Invitrogen) to the infrascapular region of the recipient mice. Mice with tumors 7-8 mm in diameter (10-12 days after inoculation) were used in the study.

When the tumors reached the size of 7-8 mm, the mice were injected i.v. via tail vein with the photosensitizers at a dose of 10 mg of Ce6 equivalent per kg body weight, dissolved in saline (0.9% NaCl solution) in the concentration of 3 mg/mL. Total volume per one injection was 100 µL.

In vivo and *ex vivo* fluorescence imaging

Epi-fluorescence imaging was performed on the IVIS-Spectrum system (Caliper Life Sciences, USA) using excitation at 640 nm (bandwidth, 30 nm) and emission at 720 nm (bandwidth, 20 nm) with 2-second exposure time. Fluorescence intensity was scaled as units of photons per second per centimeter squared per steradian ($p/s/cm^2/sr$).

First, the distribution of the PS in mice and accumulation in the tumor were assessed *in vivo* for 24 h. The images were acquired before the injection of PS (control), and 20 min, 1 h, 2 h, 3 h, 4 h, 6 h, and 24 h after. Before imaging, the mice were shaved to reduce light scattering and autofluorescence. During the image processing, the tumor and normal tissue on the leg were chosen as regions of interest (ROIs). The average fluorescence intensity (FI) in those ROIs was quantified in Living Image 2.5 software and normalized to its corresponding value measured before the injection.

In vivo fluorescence imaging was also carried out before the extraction of the PS to monitor PS uptake in the tumor. At the end of the imaging study, the animals were euthanized, and the tumors and normal organs were removed and their fluorescence was examined at the same settings. The average fluorescence intensity in the tumors *ex vivo* was measured, and compared with absolute PS concentration.

Kinetics of plasma drug level

Simultaneously with *in vivo* imaging, blood (25 µl) was collected from the retro-orbital sinus with a heparinized capillary tube at the time points 5-30 min, l h, 2 h, 3 h, 4 h, 5 h, 6 h, and centrifuged at 1500 rpm for 15 min to prepare plasma. Then 10 µL of the plasma was sampled and dissolved in 2 mL of sterile saline. Ce6 fluorescence in the plasma samples was analyzed by spectrofluorometry (Shimadzu RF-5301PC) (excitation at 405 nm, emission was scanned from 550-680 nm). The content of Ce6 was determined by comparison of the relative fluorescence intensities at the wavelength of 662 nm with values obtained from the calibration curve constructed for each formulation. To construct calibration curves, a known amount of the PS in plasma was added in sterile saline. Before the calibration, 10 µL PS formulation was mixed with 200 µL PS-free mouse plasma to avoid the influence of the PS interaction with plasma proteins on the fluorescence intensity when evaluating the concentration.

Chemical extraction

For the detailed biodistribution analysis, 4 h after injection the mice were sacrificed, and the tumor, lung, heart, brain, liver, spleen, stomach, pancreas, small intestine, kidneys, bladder, ovaries, skin, and muscle were harvested, rinsed in 0.9% NaCl, and weighed. Tissue samples of 100 mg were homogenized with Tissue Ruptor (QIAGEN), suspended in 3 mL NaOH (1mol/L)/0.3% SDS and kept in the dark at room temperature for 1 h.

The tissue extracts were analyzed by spectrofluorometry (Shimadzu RF-5301PC). Fluorescence was excited at 405 nm, and scanned from 550 to 680 nm. The content of Ce6 in the samples was determined by comparison of the relative fluorescence intensities at the wavelength of 662 nm with values obtained from the calibration curve.

The calibration curves were obtained from known amounts of the PS in tissue samples from uninjected mice dissolved in NaOH (1 mol/L)/0.3% SDS. Separate calibration curves were constructed for each tissue type or organ, and the value of the emission of the endogenous fluorophores at 662 nm was set to zero. To avoid the influence of tissue autofluorescence, including that of chlorin-like metabolites, on the results of extraction, the mean of emission values at 662 nm for each specific tissue sample from three uninjected mice was determined and subtracted from corresponding value of tissue extracts.

The results were expressed as μg Ce6 equivalent per gram tissue.

Statistical methods

The results are presented as means (M) and standard deviations (SD).

Statistical analysis was conducted using STATISTICA 10 software package. The one-way ANOVA with Tukey's *post-hoc* test was used to establish the significance of differences between groups. Differences were considered statistically significant when $P<0.05$.

Pearson's correlation coefficient (r) was calculated to determine the correlation between tumor fluorescence and absolute Ce6 concentration.

Results

In vivo fluorescence imaging of PS

Fluorescence imaging of CBA mice bearing mouse cervical carcinoma s.c. on a shoulder was performed after systemic administration of Ce6, its complexes with amphiphilic polymers PVP, PVA, and F108, and PDZ. Figure 1A shows representative *in vivo* fluorescence images of the mice before (control) and at different time-points after intravenous injection of the PS. Quantification of the signal in tumor (T) and normal tissue (N) area on the thigh was performed (Figure 1B) to further calculate T/N ratio that reflects selectivity of the PS to the tumor. Within 20 min post-injection of all the PS an intensive fluorescence was detected across the whole animal body indicating the PS circulation in the blood stream, uptake in the skin and the abdominal organs. For all preparations, except PDZ, maximum fluorescence in the tumor area was observed already at the first time-point (20 min), persisted to be highest until 1 h post-injection for Ce6 and Ce6-PVA and until 2 h post-injection for Ce6-PVP and Ce6-F108, and then decreased slowly. Accumulation and retention of the PS in the tumor allowed distinguishing the tumor from surrounding tissues starting from 3 h. In normal tissue areas fluorescent signal gradually decreased from 1 h after injection. In case of PDZ, most intensive fluorescence both in the tumor and normal tissue was observed from 1 to 4 h post-injection.

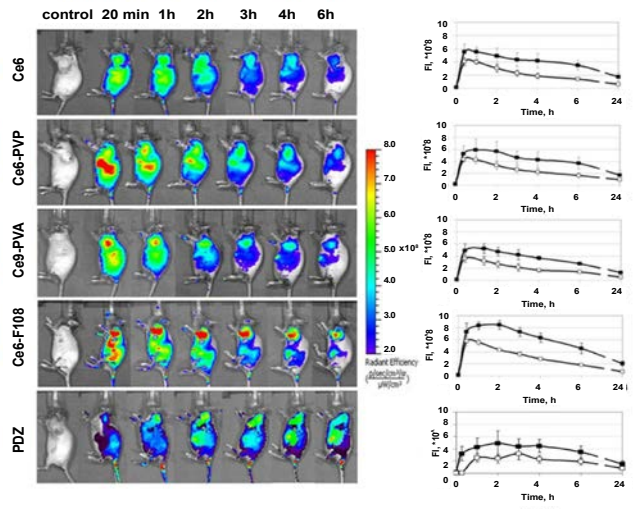

Figure 1: *in vivo* monitoring of fluorescence signal distribution after i.v. injection of Ce6 and its complexes with PVP, PVA and F108, and PDZ into CBA mice with the s.c. mouse cervical carcinoma. A – serial fluorescence images of mice (ex. 640 nm, detection 720 nm), B – quantification of the fluorescence signal (FI) in the tumor (■) and normal tissues (□). FI values at selected time point after injection were normalized to its corresponding value measured before the injection. Data are expressed as mean ± SD (n = 3 mice per group).

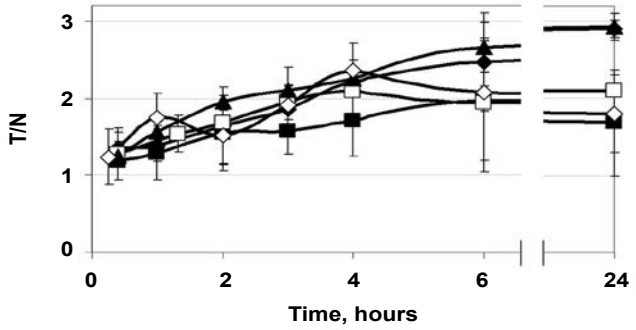

Figure 2: Time course of T/N after intravenous injection of Ce6 (♦), Ce6-PVP (■), Ce6-PVA (□), Ce6-F108 (▲), and PDZ (◊) into CBA mice with the s.c. mouse cervical carcinoma. Data are expressed as mean ± SD (n = 3 mice per group).

Slower removal of the PS from the tumor than from normal tissues resulted in the gradual growth of the T/N curves (Figure 2). T/N ratios increased from 1.2 at the 20 min time-point to 2 for Ce6-PVP, Ce6-PVA, and PDZ or to 2.5 for Ce6 and Ce6-F108 at 6 h post-injection, however, the differences between all the groups in T/N values during this period were statistically insignificant. 24 h post-injection T/N values of Ce6-PVP and PDZ decreased to 1.68, Ce6-PVA did not change, and Ce6 and Ce6-F108 increased to 2.9. Statistically significant difference was observed between the groups Ce6 and Ce6-PVP ($p=0.006$), Ce6 and PDZ ($p=0.012$), Ce6-F108 and PDZ ($p=0.017$), Ce6-PVA and Ce6-F108 ($p=0.008$), at the 24 h time-point.

Plasma concentration analysis

The levels of Ce6 in mouse plasma at various times after i.v. administration (10 mg/kg) of PDZ, free Ce6 and different formulations are presented in Figure 3. Essential differences were observed in the kinetic curves during 4 hours after injection. The plasma concentration of Ce6-PVA and Ce6-F108 declined exponentially. Ce6-PVA showed faster clearance from bloodstream at early time-points. Ce6-PVP displayed maximum concentration in plasma (9.1 ± 2.5% ID) at 1-hour post-injection, and then the concentration gradually decreased. A delayed peak of concentration (10.4 ± 3.8% ID in 2 h after injection) was typical for PDZ. More prolonged circulation in plasma was detected for free Ce6. Its concentration fell down to 16.7 ± 3.9% ID for

the first 30 min, and further the curve exhibited a shoulder in a descent phase. By 4 h post-injection, the plasma level of PS did not exceed 3% ID for all the formulations.

Tissue uptake analysis

Based on the data of *in vivo* fluorescence imaging and drug kinetics in plasma, the 4-hour time-point was chosen for detailed biodistribution study. At this time, the fluorescence of the tumors and the T/N ratios were still at the high level indicating accumulation of the PS in the tumor, while the concentration of the PS in plasma was low indicating removal from the blood and uptake in tissues.

The absolute amount of Ce6 in various tissues was determined by chemical extraction and spectrofluorimetry. Ce6 content in the tumor and normal tissues 4 h after intravenous injection is summarized in Table 1.

The intestine and/or feces had the highest concentrations of Ce6 in all cases that pointed to the primary excretion route. It was noticed that the total amount of the PS in the intestine and feces was much less for Ce6 – PVA and Ce6 - F108, presumably due to faster elimination from the body. The quantity of the extracted Ce6 in the liver, lung, stomach, pancreas and kidneys varied strongly for different preparations. The lowest content of PS was found in the muscles, heart, brain and ovaries. All polymeric complexes reduced concentration of Ce6 in the skin compared to free Ce6 and PDZ, which is important from the point of view of skin photosensitivity. Most essential decrease was revealed for Ce6-PVP (by a factor of 6.5 and 7.7 correspondingly).

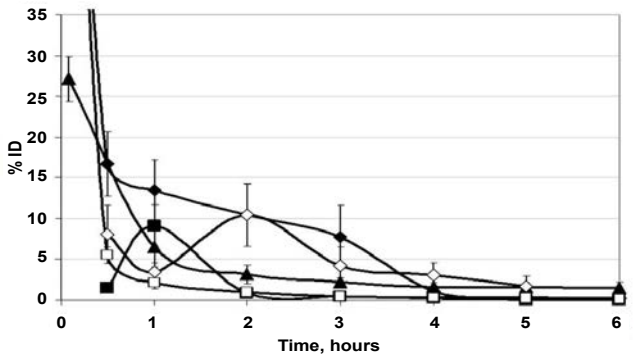

Figure 3: Concentration of Ce6 in plasma as a function of time after intravenous injection of Ce6 (♦), Ce6-PVP (■), Ce6-PVA (□), Ce6-F108 (▲), and PDZ (◊) into CBA mice with the s.c. mouse cervical carcinoma. Data are expressed as mean ± SD (n = 3 mice per group).

The results showed that the mean concentration of Ce6 extracted from tumor nodules was highest for free Ce6 (6.50 ± 0.85 μg/g tissue). Concentrations of Ce6 formulated with three different polymers were comparable with clinically used photosensitizer Photoditazine (1.94 ± 0.73 μg/g tissue), but generally lower than that of free Ce6.

Based on the extraction data, tumor-to-skin and tumor-to-muscle ratios were calculated to estimate selectivity of the PS (Table 2). In spite of the notable difference in absolute concentrations of Ce6 and its polymeric complexes in the tumor tissue, there was no difference in tumor-to-skin ratios that amounted to about 3.7. The largest tumor-to-muscle ratio was found for free Ce6 (46.89 ± 17.77). Polymeric formulation reduced the ratio by a factor of 6.9 (PVP), 5.9 (PVA), and 6.2 (F108). PDZ had the lowest ratios (0.69 ± 0.09 for skin, 1.52 ± 0.20 for muscles) at the chosen 4 hour time-point.

The absolute concentration of Ce6 in the tumor was found to have a strong correlation with tumor fluorescence *ex vivo*; Pearson's correlation (*r*) values were 0.93, 0.83, 0.94, 0.85, and 0.91 for free Ce6, Ce6-PVP, Ce6-PVA, Ce6-F108, and PDZ respectively. No correlation of the absolute concentration and *in vivo* fluorescence was found presumably because of the strong attenuation of the tumor fluorescence by the overlaying skin.

Discussion

In the present study, we have investigated the effect of amphiphilic polymers on the tissue distribution of Ce6 in tumor-bearing mice, and made a comparison with clinically used photosensitizer Photoditazine.

Tissue	Ce6	Ce6 - PVP	Ce6 - PVA	Ce6 - F108	PDZ
Intestine	203.04 ± 85.46	234.78 ± 91.35[b]	32.75 ± 11.24[a]	18.18 ± 9.93[a]	109.15 ± 31.4
Feces	321.47 ± 123.54	349.61 ± 104.8	85.64 ± 19.07[a]	7.82 ± 1.34[a]	186.71 ± 71.52
Tumor	6.50 ± 0.85[c]	1.03 ± 0.11	1.71 ± 0.54	2.52 ± 0.86	1.94 ± 0.73
Liver	2.04 ± 0.29[b]	5.23 ± 1.30	4.85 ± 1.49	3.57 ± 1.12	5.42 ± 1.58[a]
Stomach	0.75 ± 0.29	9.71 ± 4.18c	2.57 ± 1.12	0.59 ± 0.09	0.45 ± 0.06
Lung	3.36 ± 0.70	2.32 ± 0.57	6.83 ± 2.66	9.46 ± 1.33a	5.47 ± 1.90
Kidneys	1.11 ± 0.36	7.33 ± 0.73[c]	1.06 ± 0.37	0.86 ± 0.20	1.48 ± 0.37
Pancreas	0.34 ± 0.15[b]	1.02 ± 0.11[a]	0.18 ± 0.05[b]	1.21 ± 0.19[a]	0.89 ± 0.09[a]
Spleen	1.98 ± 0.79	1.09 ± 0.41	1.82 ± 0.59	1.78 ± 0.63	1.43 ± 0.25
Skin	1.76 ± 0.25	0.27 ± 0.02[a]	0.43 ± 0.10[a]	0.82 ± 0.23	2.77 ± 0.85
Muscles	0.15 ± 0.05	0.16 ± 0.06	0.27 ± 0.11	0.35 ± 0.08	0.84 ± 0.23c
Heart	0.83 ± 0.35	1.16 ± 0.44[b]	0.33 ± 0.10	1.19 ± 0.36[b]	0.29 ± 0.06
Brain	0.03 ± 0.01	0.14 ± 0.04[a]	0.03 ± 0.01	0.09 ± 0.02[a]	0.08 ± 0.01
Ovaries	0.21 ± 0.10	0.27 ± 0.07	0.13 ± 0.05	0.16 ± 0.05	0.20 ± 0.05

Table 1: Concentration of Ce6 in tumor and normal tissues 4 h after i.v. injection in CBA mice at a dose of 10 mg/kg. Values are expressed in μg/g of tissue and given as means ± SD (n = 4). Lower case letter [a]denotes statistically significant difference (P<0.05) between marked and Ce6 groups, [b] – between marked and PDZ groups, [c] – between marked and all the other groups.

	Ce6	Ce6-PVP	Ce6-PVA	Ce6-F108	PDZ
Tumor:skin ratio	3.74 ± 0.64	3.78 ± 0.09	3.78 ± 1.34	3.12 ± 0.46	0.69 ± 0.09[c]
Tumor:muscle ratio	46.89 ± 17.77[c]	6.74 ± 2.17	7.91 ± 2.74	7.50 ± 1.78	1.52 ± 0.20

Table 2: Tumor to normal tissue ratios of Ce6 4 h after i.v. injection in CBA mice with s.c. mouse cervical carcinoma. Means ± SD (n = 4). The means of the ratios from individual mice are presented. Lower case letter cdenotes statistically significant difference (P<0.05) between marked group and all the other groups.

Various polymeric carriers have been shown to improve solubility, photophysical properties, phototoxicity, cellular uptake and pharmacokinetics of hydrophobic PS [6-19]. However, the polymer-based formulations have not been fully investigated and have not found wide application in PDT. *In vivo* studies are especially limited. Most studies include one PS-polymer complex and free PS as a control. As researchers use different tumor models and different experimental conditions (drug doses, composition, administration route, methods of PS quantification, treatment parameters), it is hard to compare different PS-polymer complexes and estimate their real applicability for fluorescence diagnostics and PDT.

Fluorescence whole-body imaging has been widely applied in biomedical studies owing to the possibility of *in vivo* non-invasive longitudinal monitoring of exogenous fluorescence in small animals [24]. The advantages of the fluorescence imaging can be used for analysis of distribution and tumor targeting of new PSs for PDT, as it was shown in references [25,26]. We used the method to assess kinetics of the PS uptake in the tumor and removal from normal tissues. Quantification of the fluorescence intensity in the tumor and normal tissues *in vivo* did not reveal any significant differences in the fluorescence kinetics of the formulations with polymers and free Ce6. Shi et al. studied accumulation of Ce6 in the s.c. H-22 mouse tumor *in vivo* by means of fluorescence imaging and showed that Ce6 uptake in the tumor reached a maximum 2 h after i.v. injection (25 mg/kg) and slowly washed out over time [27]. In our study the maximum was 20 min, but the curve shapes were similar. The difference in times is likely to be related to the lower dose of Ce6 (10 mg/kg) used in our study. Earlier we analyzed dose-dependent pharmacokinetics of Photodithazine in a mouse cervical carcinoma *in vivo* using fluorescence transillumination imaging and demonstrated faster kinetics of accumulation for lower PS doses [28].

The results of the chemical extraction of the PSs from normal tissues obtained in this study agreed well with other works, where Ce6 and its polymer-based formulations were tested. For instance, Chin et al. [9] also detected the highest amount of Ce6 from free Ce6 and Ce6–PVP in the small and large intestines as they are the main routes for drug removal from the body, and the amount of drug was comparable in all the organs for Ce6 and Ce6–PVP in the period 1-6 h post-injection [9]. Upon *ex vivo* evaluation of excised tissues 4 h after injection the strongest fluorescence of Ce6 was shown in the liver, intestine, stomach and skin, and the lowest – in the muscle, heart and cerebrum [27]. 72 h after i.v. injection, Park et al. found the most intensive Ce6 fluorescence in the liver, lung and kidney (fluorescence in the intestine was not measured) [14].

We analyzed concentration of Ce6, its modified forms and PDZ in blood plasma during 6 h post-injection and revealed marked differences in the kinetics curves. Pharmacokinetic profiles of only Ce6-PVA and Ce6-F108 were described by a standard bi-exponential decline of the drug concentration.

Ce6-PVP and PDZ showed a delayed maximum plasma level. Such an unusual pharmacokinetic profile was also found for the hydrophobic photosensitizer *meso*-tetra-hydroxyphenyl-chlorin (mTHPC) in humans [29]. Possible explanation for the delayed plasma peak is the formation of a drug depot in the excretory organs immediately after i.v. injection with subsequent release back into the circulation. Another possible reason can be aggregation and precipitation of PS in the vascular compartment followed by interaction with plasma proteins and disaggregation. However, this contradicts the currently accepted concept that PVP prevents aggregation of PS. There are experimental data indicating that Ce6-PVP remains stable in plasma and reaches the tumor either as a Ce6–PVP complex or as a ternary Ce6–PVP–HSA complex [11]. Additionally, Ce6–PVP was found to interact more with very low-density lipoproteins in comparison to Ce6 alone [10]. In the study by Wen et al. Photoditazine concentration in serum exponentially decreased without a delayed peak, but general rate of PS elimination from blood looks similar to that in our research [30]. Therefore, the mechanisms of the pharmacokinetic behavior of Ce6–PVP and PDZ in bloodstream are not fully understood.

The slowest decline was found for free Ce6 that is supposed to be a result of direct interaction with plasma proteins. The major carrier for Ce6 in plasma is albumin, and to a lower extent, low-density lipoproteins. According to Cunderlikova et al. [31] about 90% of Ce6 in human plasma and 75% in fetal calf serum is bound to albumin.

The affinity of Ce6 for lipoproteins increases at low pH that may be important for intracellular uptake in the acidic tumor environment [32]. Similarly to our data, Shi et al. [27] observed gradual decrease of the Ce6 concentration in plasma between 0.5 and 4 h post-injection. We assume that higher accumulation of Ce6 in tumor in comparison with polymeric compositions and PDZ most likely resulted from prolonged circulation in blood.

There are a few studies demonstrating enhanced tumor uptake of polymer-based substances of PS. Hamblin et al. [6] reported that pegylation of a Ce6 poly-l-lysine conjugate gave higher amounts of PS in tumor and higher tumor:normal tissue ratios after intraperitoneal (i.p.) injection into nude mice bearing i.p. ovarian cancer OVCAR-5. In the studies by Chin et al. PVP greatly enhanced Ce6 concentration in subcutaneous (s.c.) human bladder carcinoma xenografts MGH, compared with Ce6 alone, and increased the therapeutic index of PDT without any side effects upon i.v. administration [9]. In another work of Chin's group the comparative efficacy of PDT with Ce6-PVP in treating non-small cell lung carcinoma (NSCLC) and small cell lung carcinoma (SCLC) was evaluated. Ce6-PVP showed greater tumor necrosis against human NSCLC xenografts in nude mice following irradiation compared to SCLC [8]. Recently, Park et al. [14] found that conjugation of Ce6 to pluronic F127 exhibited enhanced tumor-specific distribution and tumor growth inhibition after i.v. injection into nude mice with s.c. colon cancer CT-26. Brasseur et al. [5] have studied pharmacokinetics of aluminium phthalocyanine (AlClPc) conjugated via an axial coordination bond to PVA or PEG in the EMT-6 tumour-bearing mice. AlPc–PVA exhibited the highest tumor-to-skin and tumor-to-muscle ratios as well as the highest and most persistent tumor uptake. Hypericin-PVP complex is being extensively investigated in the experiments *in vitro* and *in vivo* and clinical trials and demonstrate great potential as a diagnostic and therapeutic agent [33,34]. The most common explanation for these results is connected with the longer plasma circulation time of the polymeric complexes.

Besides an enhanced accumulation in tumor, some other factors play an important role in improving diagnostic and therapeutic properties of PS-polymer formulations. For example, Davis et al. [12] have carried out *in vivo* assay of distribution properties of benzoporphyrin derivative conjugated to modified PVA (M-PVA-BPD) in comparison with free BPD. It was found that the level of M-PVA-BPD in rhabdomyosarcoma M1 of DBA2 mice was lower than that of free BPD, but the conjugate was bound more tightly to the tumor cells and affected higher tumor cell kill when activated by light. In addition, polymeric formulations are easy to prepare and provide an efficient solubilization of hydrophobic Ce6. *In vitro* studies show enhanced phototoxicity of the polymer-formulated Ce6 against

cancer cells owing to disaggregation and higher singlet oxygen yield [19,34,35]. Taken together, these results testify to the potential usability of the Ce6-polymer formulations in PDT.

In our study, the polymers PVA, PVP, and pluronic F108 did not increase an uptake of Ce6 in the mouse cervical carcinoma. In case of polymeric compositions, quantity of chlorin in the tumor tissue did not differ from Photoditazine. Although absolute concentration of the polymer-formulated PS in the tumor was lower than that of Ce6 alone, tumor-to-skin ratios were similar. It is essential that Ce6-polymer complexes exhibited better selectivity to the tumor than Photoditazine at the selected time-point. Our data about accumulation of Photoditazine in the tumor to a lesser degree than in skin after i.v. injection of 10 mg/kg agreed well with reference [30], where biodistribution of the PS was studied in mice bearing HPV 16 E6/E7 associated cervical cancer. Lower accumulation in the skin (especially for Ce6-PVP) and faster elimination from the body (Ce6-PVA, Ce6-F108) in comparison with Ce6 along and Photoditazine seem important for overcoming the problem of normal tissue photosensitivity. Less phototoxic effect of the Ce6-PVP formulation compared to Ce6 alone in skin of nude mice was shown by Chin et al. [7]. Since PS accumulation in a tumor is always a balance between the uptake rate and the blood concentration as well as the liver clearance, it cannot be excluded that biodistribution analysis at earlier time-points or the use of other tumor model might show larger quantity of PS in tumor tissue and better selectivity.

Conclusion

The study was carried out to test the ability of three Ce6-polymer conjugates to target the tumor. Mouse cervical carcinoma inoculated subcutaneously in mice was used as a tumor model. The results showed that none of the polymers significantly changed fluorescence kinetics in the tumor. It is important that concentration of the Ce6 formulated with polymers in the tumor tissue was comparable with clinically used photosensitizer Photoditazine, but uptake in the skin was less. At the same time, tumor-to-skin ratios of the Ce6-polymer complexes were similar to free Ce6. We concluded that the use of the polymeric formulation is reasonable for fluorescence diagnosis and PDT of cancer.

Acknowledgement

This work was supported by the Ministry of Education and Science of the Russian Federation (project No. 11.G 34. 31.0017) and the Russian Foundation for Basic Research (projects # 11-02-01090, 14-02-00738).

References

1. Dolmans DE, Fukumura D, Jain RK (2003) Photodynamic therapy for cancer. Nat Rev Cancer 3: 380-387.
2. Agostinis P, Berg K, Cengel KA, Foster TH, Girotti AW, et al. (2011) Photodynamic therapy of cancer: an update. CA Cancer J Clin 61: 250-281.
3. O'Connor AE, Gallagher WM, Byrne AT (2009) Porphyrin and nonporphyrin photosensitizers in oncology: preclinical and clinical advances in photodynamic therapy. Photochem Photobiol 85: 1053-1074.
4. Gijsens A, De Witte P (1998) Photocytotoxic action of EGF-PVA-Sn(IV)chlorin e6 and EGF-dextran-Sn(IV)chlorin e6 internalizable conjugates on A431 cells. Int J Oncol 13: 1171-1177.
5. Brasseur N, Ouellet R, La Madeleine C, van Lier JE (1999) Water-soluble aluminium phthalocyanine-polymer conjugates for PDT: photodynamic activities and pharmacokinetics in tumour-bearing mice. Br J Cancer 80: 1533-1541.
6. Hamblin MR, Miller JL, Rizvi I, Ortel B, Maytin EV, et al. (2001) Pegylation of a chlorin(e6) polymer conjugate increases tumor targeting of photosensitizer. Cancer Res 61: 7155-7162.
7. Chin WW, Lau WK, Heng PW, Bhuvaneswari R, Olivo M (2006) Fluorescence imaging and phototoxicity effects of new formulation of chlorin e6–polyvinylpyrrolidone. J Photochem Photobiol B 84: 103-110.
8. Chin WWL, Heng PWS, Olivo M (2007) Chlorin e6 – polyvinylpyrrolidone mediated photosensitization is effective against human non-small cell lung carcinoma compared to small cell lung carcinoma xenografts. BMC Pharmacology 7: 15.
9. Chin WW, Heng PW, Thong PS, Bhuvaneswari R, Hirt W, et al. (2008) Improved formulation of photosensitizer chlorin e6 polyvinylpyrrolidone for fluorescence diagnostic imaging and photodynamic therapy of human cancer. Eur J Pharm Biopharm 69: 1083-1093.
10. Chin WW, Praveen T, Heng PW, Olivo M (2010) Effect of polyvinylpyrrolidone on the interaction of chlorin e6 with plasma proteins and its subcellular localization. Eur J Pharm Biopharm 76: 245-252.
11. Isakau HA, Parkhats MV, Knyukshto VN, Dzhagarov BM, Petrov EP, et al. (2008) Toward understanding the high PDT efficacy of chlorine e6–polyvinylpyrrolidone formulations: Photophysical and molecular aspects of photosensitizer–polymer interaction in vitro. J Photochem Photobiol B 92: 165-174.
12. Davis N, Liu D, Jain AK, Jiang SY, Jiang F, et al. (1993) Modified polyvinyl alcohol-benzoporphyrin derivative conjugates as phototoxic agents. Photochem Photobiol 57: 641-647.
13. van Nostrum CF (2004) Polymeric micelles to deliver photosensitizers for photodynamic therapy. Adv Drug Deliv Rev 56: 9-16.
14. Park H, Na K (2013) Conjugation of the photosensitizer Chlorin e6 to pluronic F127 for enhanced cellular internalization for photodynamic therapy. Biomaterials 34: 6992-7000.
15. Chowdhary RK, Sharif I, Chansarkar N, Dolphin D, Ratkay L, et al. (2003) Correlation of photosensitizer delivery to lipoproteins and efficacy in tumor and arthritis mouse models; comparison of lipid-based and Pluronic P123 formulations. J Pharm Pharm Sci 6: 198-204.
16. Hioka N, Chowdhary RK, Chansarkar N, Delmarre D, Sternberg E, et al. (2002) Studies of a benzoporphyrin derivative with Pluronics. Can J Chem 80: 1321-1326.
17. Li B, Moriyama EH, Li F, Jarvi MT, Allen C, et al. (2007) Diblock copolymer micelles deliver hydrophobic protoporphyrin IX for photodynamic therapy. Photochem Photobiol 83: 1505-1512.
18. Roby A, Erdogan S, Torchilin VP (2006) Solubilization of poorly soluble PDT agent, meso-tetraphenylporphin, in plain or immunotargeted PEG-PE micelles results in dramatically improved cancer cell killing in vitro. Eur J Pharm Biopharm 62: 235-240.
19. Zhiyentayev TM, Boltaev UT, Solov'eva AB, Aksenova NA, Glagolev NN, et al. (2013) Complexes of Chlorin e6 with Pluronics and Polyvinylpyrrolidone: Structure and Photodynamic Activity in Cell Culture. Photochem Photobiol .
20. Bae YH, Park K (2011) Targeted drug delivery to tumors: myths, reality and possibility. J Control Release 153: 198-205.
21. Istomin YP, Kaplan MA, Shliakhtsin SV, Lapzevich TP, Cerkovsky DA, et al. (2009) Immediate and long-term efficacy and safety of photodynamic therapy with Photolon (Fotolon): a seven-year clinical experience. Proc SPIE, Photodynamic therapy: back to the future 7380.
22. Istomin YP, Lapzevich TP, Chalau VN, Shliakhtsin SV, Trukhachova TV (2010) Photodynamic therapy of cervical intraepithelial neoplasia grades II and III with Photolon. Photodiagnosis Photodyn Ther 7: 144-151.
23. Kozlov AM, Sof'ina ZP (1978) Frequency, times, and type of metastasization of transplantable tumors in mice. Bulletin of Experimental Biology and Medicine 86: 1645-1647.
24. Leblond F, Davis SC, Valdés PA, Pogue BW (2010) Pre-clinical whole-body fluorescence imaging: Review of instruments, methods and applications. J Photochem Photobiol B 98: 77-94.
25. Foster TH, Giesselman BR, Hu R, Kenney ME, Mitra S (2010) Intratumor administration of the photosensitizer Pc 4 affords photodynamic therapy efficacy and selectivity at short drug-light intervals. Transl Oncol 3: 135-141.
26. Choi Y, Weissleder R, Tung CH (2006) Selective antitumor effect of novel protease-mediated photodynamic agent. Cancer Res 66: 7225-7229.
27. Shi H, Liu Q, Qin X, Wang P, Wang X (2011) Pharmacokinetic study of a novel sonosensitizer chlorin-e6 and its sonodynamic anti-cancer activity in hepatoma-22 tumor-bearing mice. Biopharm Drug Dispos 32: 319-332.

28. Shirmanova M, Zagaynova E, Sirotkina M, Snopova L, Balalaeva I, et al. (2010) *in vivo* study of photosensitizer pharmacokinetics by fluorescence transillumination imaging. J Biomed Opt 15: 048004.

29. Triesscheijn M, Ruevekamp M, Out R, Van Berkel TJ, Schellens J, et al. (2007) The pharmacokinetic behavior of the photosensitizer meso-tetra-hydroxyphenyl-chlorin in mice and men. Cancer Chemother Pharmacol 60: 113-122.

30. Wen LY, Bae SM, Do JH, Park KS, Ahn WS (2011) The effects of photodynamic therapy with Photodithazine on HPV 16 E6/E7 associated cervical cancer model. J Porphyrins Phthalocyanines 15: 174-180.

31. Cunderlíková B, Kongshaug M, Gangeskar L, Moan J (2000) Increased binding of chlorin e6 to lipoproteins at low pH values. Int J Biochem Cell Biol 32: 759-768.

32. Mojzisova H, Bonneau S, Vever-Bizet C, Brault D (2007) The pH-dependent distribution of the photosensitizer chlorin e6 among plasma proteins and membranes: a physico-chemical approach. Biochim Biophys Acta 1768: 366-374.

33. Vandepitte J, Van Cleynenbreugel B, Hettinger K, Van Poppel H, de Witte PA (2011) Biodistribution of PVP-hypericin and hexaminolevulinate-induced PpIX in normal and orthotopic tumor bearing rat urinary bladder. Cancer Chemother Pharmacol 67: 775-781.

34. Kubin A, Meissner P, Wierrani F, Burner U, Bodenteich A, et al. (2008) Fluorescence diagnosis of bladder cancer with new water soluble hypericin bound to polyvinylpyrrolidone: PVP-hypericin. Photochem Photobiol 84: 1560-1563.

35. Gorokh YuA, Aksenova NA, Solov'eva AB, Ol'shevskaya VA, Zaitsev AV, et al. (2011) The influence of amphiphilic polymers on the photocatalytic activity of water soluble porphyrin photosensitizers. Russian Journal of Physical Chemistry A 85: 871-875.

This article was originally published in a special issue, **Photodynamic Therapy- Cancer** handled by Editor. Dr. Zhiwei Hu, Yale University School of Medicine, USA